Performance of Rehabilitation Treatments for Rigid Pavements Affected by Durability Cracking

Taofeek Mustapha, MSc Candidate, University of Manitoba
Ahmed Shalaby, Ph.D., P.Eng., University of Manitoba
Ahmed Ghazy, Ph.D., P.Eng., City of Winnipeg

Paper prepared for the session

Innovative Technologies in Asset Management
2026 Transportation Association of Canada (TAC) Conference & Exhibition
Winnipeg, Manitoba

Abstract

Durability cracking (d-cracking), a progressive distress, remains a significant concern for rigid pavements. This distress can be attributed to the use of coarse aggregates from a limestone source with pore structure sizes ranging from 0.1 – 0.2 µm. The damage can be accelerated by cycles of freezing and thawing in cold weather regions and inadequate pavement drainage.

Selection of an appropriate treatment for pavements affected by d-cracking depends on the condition of the pavement and the underlayers. The treatments may include partial or full-depth repairs, overlays, asphalt patching, reconstruction, or slab stabilization. This study conducted pre- and post-treatment testing and evaluated their performance on the streets where they were applied.

A group of twelve pavement sections having varying levels of damage due to d-cracking were selected. Site visits and field survey were conducted using a falling weight deflectometer (FWD). Mid-slab tests were conducted to assess the pavement layer stiffnesses, and load transfer efficiency test was also conducted to determine the condition of load transfer devices (dowels) as well as the base support and for void detection.

The data generated were then assessed to check that the variability between loading sequences is not greater than 3% and standardize the deflection data to a 40 kN load. BAKFAA software was used to conduct backcalculations to determine the elastic modulus of each pavement layer at mid-slab and load transfer efficiency (LTE) of dowel at transverse joints. Additionally, from the automated distress survey data supplied, common distresses affecting rigid pavements were identified and their corresponding distress densities were calculated.

LTE results allowed classification of d-cracking severity levels, revealing that as d-cracking progresses, load transfer of dowel at transverse joints can also deteriorate significantly. Poor LTE shows correlation with increased risk of pumping, faulting, and accelerated distress propagation. Backcalculated modulus for each pavement layer was compared against the typical ranges. Several values fell outside and below the expected modulus threshold. The automated distress survey data showed that certain segments exhibited high distress density which can be linked to lower LTE and reduced moduli.

The results from these two sources can be compared and used to develop a decision support tool (DST) for pavement condition assessment, performance prediction, and recommending appropriate treatment. The DST will be based on comparing values from both sources to assess the condition of each pavement layer.

Therefore, this framework can provide satisfactory performance and cost-effectiveness because the selected pavement treatment will be based on data-driven pavement management system (PMS) approaches.

1.0 Introduction

Concrete is widely used because of its flexural strength and durability. However, defects such as d-cracking, alkali aggregate reaction (AAR) may be due to less quality aggregates, coarse aggregates with limestone source (Taylor and Wang, 2015), and freeze-thaw damage in frost-susceptible coarse aggregates that retain moisture within the concrete matrix (Mcleod et al., 2014). These could have significantly reduced the lifespan of some rigid pavements in some cold regions, including Winnipeg. Existing rehabilitation strategies may be optimized to achieve better expected results by tailoring solutions that adequately classify and consider the severity of distresses and environmental conditions.

1.1 The objectives and background

- Identify and assess pavement conditions before and after treatment

- Evaluate the performance of rehabilitation techniques applied to d-cracked pavements

- Develop a decision matrix for the applied rehabilitation techniques that align with the severity of d-cracking and site conditions (ongoing).

Previous studies showed that slab fracturing rehabilitation methods such as rubblization of jointed reinforced concrete pavement (JRCP) or jointed plain concrete pavement (JPCP) resulted in satisfactory performance. However, this technique may be unsuitable for residential street roadways due to their proximity to buildings and the relatively thin pavement thickness. Furthermore, interventions such as overlays, break and seat, and geosynthetic materials may only provide temporary relief, as reflective cracking can reappear from the existing pavement joints within a few years.

1.2 Research problem and scope

D-cracking mainly affects rigid pavements due to freezing and thawing cycles of frost-susceptible coarse aggregates. A significant number of residential streets in Winnipeg are constructed with concrete; some of these sections suffer from d-cracking deterioration. This damage may have significant effect on the pavement performance, raise safety concerns and increase the costs of maintenance. The severity of d-cracking may appear late towards the design life of rigid pavements. As a result, this study focuses on the residential concrete streets with age range of 35 to 54 years that have developed varying levels of damage due to d-cracking. The pilot streets are low-volume local roads with thin concrete thickness of 150 mm, and varying base and subbase thicknesses. Several treatments, such as partial or full-depth repairs, reconstruction, overlays, slab fracturing, can be applied to rescue the affected pavements. However, limited data is available on the performance of treatments applied on the residential street roadways. Thus, this study aims to address this and provide information to support why rehabilitation technique decisions can be made based on scientific proof and using comprehensive data.

The scope of study involves conducting non-destructive testing (NDT) using FWD equipment. The FWD testing was used to collect deflection data, provide insights into the structural capacity of the pavement layers and results obtained can be used to make informed decisions. The FWD testing data can be used to evaluate and manage future traffic loading through backcalculation and load transfer efficiency (LTE). Deflection data before and after treatments were collected, analyzed, and used for decision making.

Therefore, in this study we conducted falling weight deflectometer (FWD) testing on twelve (12) residential concrete sections. This study is also based on objective performance evaluation by conducting field surveys and analyzing the pre- and post-rehabilitation treatments of the selected rigid residential pavements affected by d-cracking in Winnipeg.

2.0 Literature review

2.1 Definition of d-cracking

D-cracking represents a specific type of progressive distress in concrete pavements. It is fundamentally caused by the freezing and thawing of frost-susceptible coarse aggregates containing water within the concrete structure (Mcleod et al., 2014). Taylor and Wang (2015) also described d-cracking as a progressive form of distress linked to the use of coarse aggregates from limestone source, which break apart when they become critically saturated and exposed to repeated cycles of freezing and thawing. Study by Janssen & Dempsey (1986) refers to d-cracking as a gradual deterioration of concrete pavement, typically due to repeated freeze-thaw cycles. D-cracking can also develop even if the concrete pavement has not experienced any physical loads. This defect is often traced back to source of the coarse aggregates which can also affect well-designed concrete mixes to experience d-cracking problems. Studies show that moisture and temperature are the main climatic factors that contribute to the development of d-cracking. As d-cracking advances in a rigid pavement, its capacity to bear loads and withstand deformation and cracking from repetitive traffic loads gradually reduces. Over time, this distress can result in complete structural failure of the pavement, and a loss of serviceability (Janssen & Dempsey, 1986).

2.2 Mechanisms of d-Cracking

D-cracking typically occurs in pavements and slabs on grade. It occurs through a complex mechanism involving water infiltration, freeze-thaw cycles, and aggregate properties. The process of d-cracking begins when water penetrates the aggregate through its pore structure, which may happen over extended periods during non-winter seasons. When temperatures drop and freezing occurs, water is expelled from the aggregate as ice forms and expands. If the pore structure prevents the water from exiting quickly enough, the trapped water freezes, causing expansion and cracking in both the aggregate and surrounding mortar (Taylor and Wang, 2015).
Taylor and Wang (2015) identified specific pore size ranges that make aggregates vulnerable to d-cracking deterioration.

- Aggregates with pores smaller than 0.1 µm are generally durable because water in these tiny pores does not typically freeze due to high specific surface area.
- Aggregates with large pores exceeding 0.2 µm tend to be durable because water can be easily expelled during freezing.
- The most problematic aggregates have intermediate pore sizes ranging from 0.1–0.2 µm, where surface tension restricts water movement, increasing the risk of critical saturation.

D-cracking usually originates from the lower part of the slab and gradually progresses upward due to groundwater drawn into the concrete from beneath, as well as through transverse and longitudinal joints (Taylor and Wang, 2015).

3.0 Methodology

3.1 Site visits

Joint site visits were conducted. After the visit, 12 pavement test sections exhibiting varying levels of d-cracking damage were identified for the study.

3.2 Falling weight deflectometer (FWD) data

The FWD truck shown in Figure 3.1 is mounted with a device that drops a known weight onto a circular plate (300 mm diameter) resting on the concrete pavement surface. The drop weight simulates the impact of a moving wheel load on the pavement. The weight's impact is transferred to the pavement layers through a circular plate that distributes the load evenly over an area. The number of locations where the weight was dropped along the network was based on the roadway length. The sensors (geophones) were arranged at a radial distance from the center of the load plate, as shown in Figure 3.2. The FWD measures the vertical deflection of the concrete surface at predefined distances from the load plate shown in Figure 3.2. The deflection data were checked to exclude data with variability between loading sequences from the same heights does not exceed 3% for any sensor (ASTM-D4694-90, 2020).

3.3 BAKFAA software for analysis

The drops from FWD testing can produce different load levels, such as 37.56, 39.20, 50.95, 69.10, 70.9 kN. To ensure consistency and comparability, the load deflection data was normalized to a 40 KN load, and the pavement structures were modelled. The analysis was conducted using the FAA BAKFAA software. The typical pavement structure was assumed to consist of three layers. The top layer, jointed plain concrete pavement (JPCP) was assumed to contain dowelled bar with thickness of 150 mm, followed by base layer of 75 mm thickness on top of the subgrade. The analysis used seed (initial) modulus values of 27,000 MPa, 135 MPa, and 30 MPa for the concrete, base, and subgrade layers, respectively. Table 3.1 shows the LTE criteria that were adopted for measuring the joint transfer performance of the pavements.

3.4 Automated distress survey data

Automated in-service pavement distress survey data collected in 2024 was provided. The data for each pavement surveyed show features such as location, segment length, slab counts, and potential pavement distress of each street. From the survey data, distresses that can affect rigid pavements were identified, severity level of each distress was noted, and the affected slabs were counted and reported.

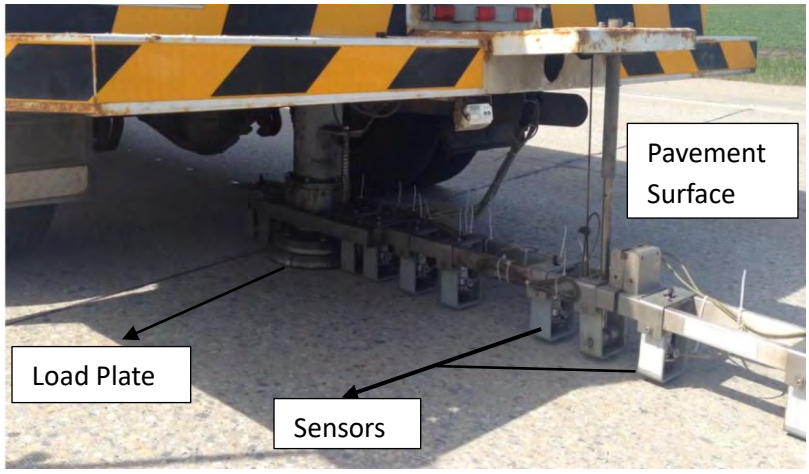

Figure 3.1: FWD truck with load plate, sensors and testing equipment

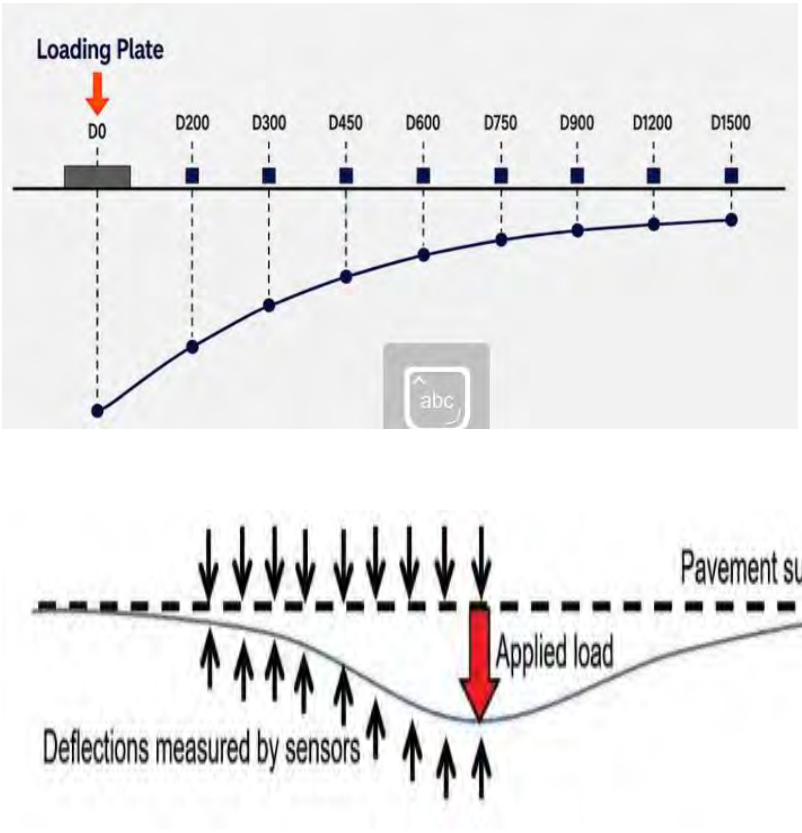

Figure 3.2: Typical FWD loading and measurement layout (FHWA, 2019).

Table 3.1**:** LTE performance criteria and corresponding expected d-cracking severity level

LTE Score (%)	LTE Scale	Expected D-cracking Severity Level	D-cracking Scale (slab area coverage)
90 -100	Excellent	Very low	-
75 - 89	Good	Low	Less than 15 percent
50 – 74	Fair	Moderate	More than 15 percent or less than 15 percent with loose or missing pieces
25 – 49	Poor	High	More than 15 percent with most pieces out or easily be removed
0 - 24	Very poor	Very high	-

Source: FHWA (2017) and USACERL (1997).

4.0 Assessment and performance results (pre- and post-treatment)

The results presented below are for the three streets where pre- and post-rehabilitation treatments have been conducted. Table 4.1 provides summary of all the Streets details, including segment length, width, pavement age, surface type and the applied treatments.

Table 4.1: Summary of the streets and the rehabilitation treatments applied

Location	Length (m)	Width (m)	Age (yrs)	Surface Type	Treatment (s) Applied
Street 1	657	7.2	41	Rigid	80 mm asphalt overlay consist of 40 mm MS2 and 40 mm MS1. Glass grid was embedded in between the two asphalt lifts along most of the street.
Street 2	511	6.9	48	Rigid	Minor rehabilitation
Street 3	206	7.0	37	Rigid	Full depth repair of a mid slab, a joint and 50 mm asphalt overlay

4.1 Street 1

Table 4.2 highlights the LTE results, pre- and post- performance rating, and the improvement level associated with each criterion. Table 4.3 presents the pre- and post-mid-span backcalculated modulus for each pavement layer, typical range, and an indicator showing whether each layer falls within or outside the range. Table 4.4 lists the identified distresses, affected slabs, and distress density based on the automated distress survey data. Figure 4.1 shows the comparison of pre- and post-rehabilitation of joints with their respective LTE values. Figure 4.2 illustrates the deflection basin graph, showing the deflection response corresponding to sensor distance from the center of the load plate. Figure 4.3 displays typical photographs of the pre- and post-joint and mid-slab pavement locations where the deflection data were collected.

Table 4.2**:** Load transfer efficiency (LTE) of before and after rehabilitation treatment

Location	**Pre-LTE Score (%)**	**Pre-Performance Rating**	**Post-LTE Score (%)**	**Post - Performance Rating**	**Level of Improvement (%)**
Joint 1	79	Good	100	Excellent	+21
Joint 2	66	Fair	74	Fair	+8

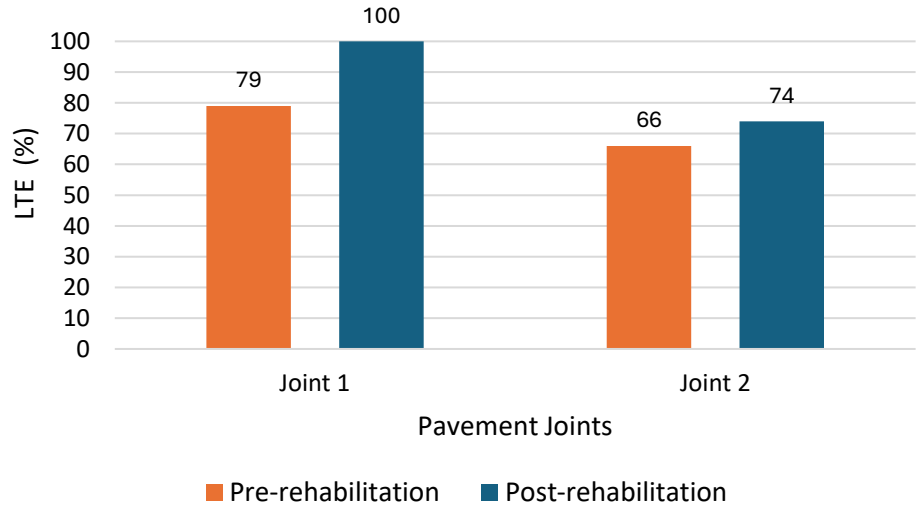

Figure 4.1: Street 1 pre- and post- LTE values at transverse joints

Table 4.3**:** Mid-slab backcalculated layer properties for pre- and post-rehabilitation treatments

Location	Layer	Thickness (mm)	Backcalculated Modulus (MPa)	Typical Range (MPa)	Backcalculation within Tolerance
Pre-rehabilitation Values					
Panel A	Rigid slab	150	24,400	20,000 - 35,000	Yes
	Base	75	193	100 - 350	Yes
	Subgrade	0	75	20 - 80	Yes
Panel B	Rigid slab	150	26,200	20,000 - 35,000	Yes
	Base	75	206	50 - 150	Yes
	Subgrade	0	55	20 - 80	Yes
Post-rehabilitation Values					
Panel A	HMA	80	3,000	1,500 – 3,500	Yes
	Rigid slab	150	24,400	20,000 - 35,000	Yes
	Base	75	229	100 - 350	Yes
	Subgrade	0	78	20 - 80	Yes
Panel B	HMA	80	3,000	1,500 – 3,500	Yes
	Rigid slab	150	29,100	20,000 - 35,000	Yes
	Base	75	286	100 - 350	Yes
	Subgrade	0	58	20 - 80	Yes

***** Out of typical range ** Below typical range

Table 4.4**:** Distresses identified on Street 1 from the automated distress survey

Distress Type	Severity Level	Count of affected Slabs (out of 108)	Distress Density (%)
Durability (D) cracking	L	8	7
	M	51	47
	H	27	25
Faulting	L	46	43
	M	20	19
	H	2	2
Divided slab	L	5	7
	M	12	11
	H	-	-
Linear cracking	L	52	48
	M	14	13
	H	-	-
Joint spalling	L	8	7
	M	49	45
	H	-	-
Corner spalling/ breaking	L	2	2
	M	3	3
	H	-	-

L – low, M - moderate, H – high

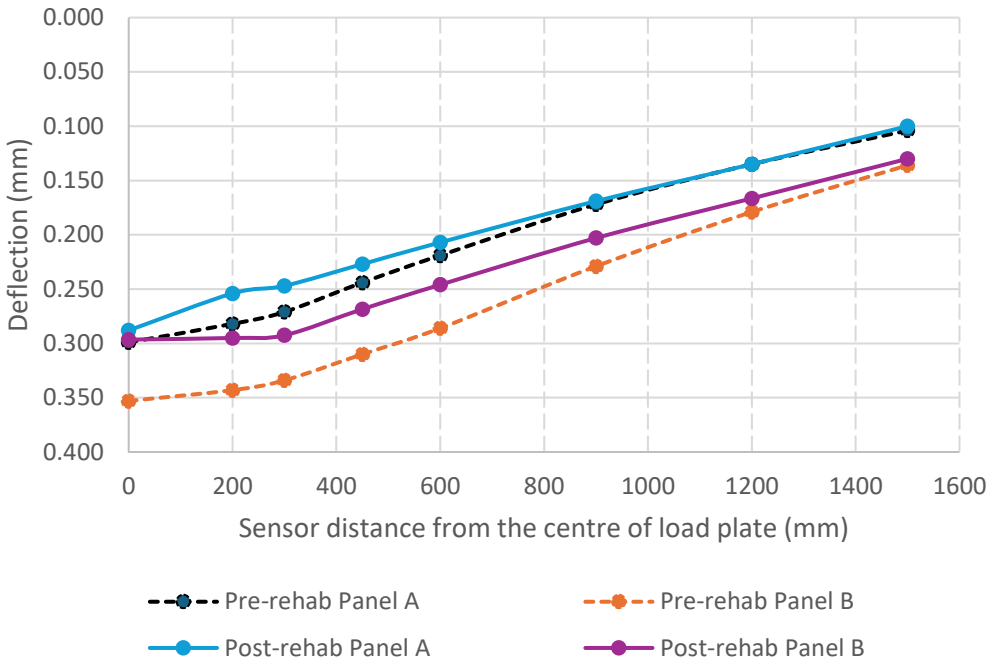

Figure 4.2: Street 1 mid-slab for pre- and post-deflection basin graph



(a) Joint Pre-rehabilitation



(b) Joint Post-rehabilitation



(c) Mid-slab panel B: Pre-rehabilitation



(d) Mid-slab panel B: Post-rehabilitation

Figure 4.3: Typical Street 1 joints and mid-slab panels of pre- and post-rehabilitation

4.2 Street 2

Table 4.5 highlights the LTE results pre- and post- performance rating, and the improvement level associated with each criterion. Table 4.6 presents the mid-span of the pre- and post-rehabilitation backcalculated modulus for each pavement layer, the corresponding typical range, and an indicator showing whether each layer falls within or outside the range. Table 4.7 lists the identified distresses, affected slabs, and distress density based on the automated distress survey data. Figure 4.4 shows the comparison of pre- and post-rehabilitation of joints with their respective LTE values. Figure 4.5 illustrates the deflection basin graph, showing the pre- and post-rehabilitation deflection response corresponding to sensor distance from the center of the load plate. Figure 4.6 presents photographs of the typical joint and mid-slab locations where the deflection data were collected.

Table 4.5: Load transfer efficiency (LTE) of before and after rehabilitation treatment

Location	Pre-LTE Score (%)	Pre-Performance Rating	Post-LTE Score (%)	Post - Performance Rating	Level of Improvement (%)
Joint 1	80	Good	96	Excellent	+16
Joint 2	75	Good	89	Good	+14

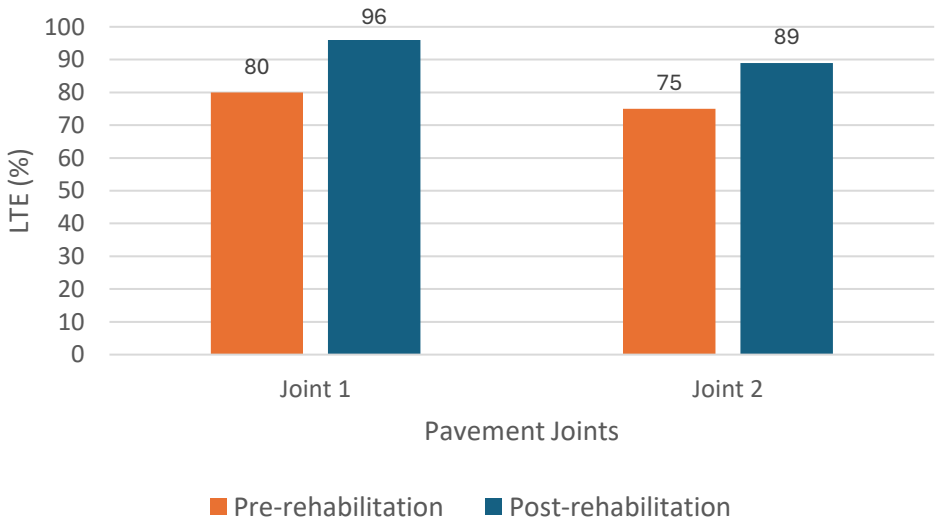

Figure 4.4: Street 2 pre- and post-LTE values at transverse joints

Table 4.6: Mid-slab backcalculated layer properties for pre- and post-rehabilitation treatment

Location	Layer	Thickness (mm)	Backcalculated Modulus (MPa)	Typical Range (MPa)	Backcalculation within Tolerance
Pre-rehabilitation values					
Panel A	Rigid slab	150	27,800	20,000 - 35,000	Yes
	Base	75	260	100 - 350	Yes
	Subgrade	0	75	20 - 80	Yes
Panel B	Rigid slab	150	46,400*	20,000 - 35,000	No
	Base	75	306	100 - 350	Yes
	Subgrade	0	92*	20 - 80	No
Pre-rehabilitation values					
Panel A	HMA	50	3,000	1,500 – 3,500	Yes
	Rigid slab	150	26,200	20,000 - 35,000	Yes
	Base	75	231	100 - 350	Yes
	Subgrade	0	104*	20 - 80	No
Panel B	HMA	50	3,000	1,500 – 3,500	Yes
	Rigid slab	150	44,600*	20,000 - 35,000	No
	Base	75	251	100 - 350	Yes
	Subgrade	0	89	20 - 80	No

***** Out of typical range ** Below typical range

Table 4.7: Distresses identified on Street 2 from the automated distress survey

Distress Type	Severity Level	Count of Affected Slabs (out of 110)	Distress Density (%)
Durability (D) Cracking	L	74	67
	M	10	9
	H	-	-
Faulting	L	50	45
	M	28	25
	H	11	10
Divided Slab	L	3	3
	M	2	2
	H	-	-
Linear Cracking	L	53	48
	M	9	8
	H	1	1
Joint Spalling	L	12	11
	M	4	4
	H	-	-
Corner Spalling/ Breaking	L	50	45
	M	3	3
	H	-	-

L – low, M - moderate, H – high

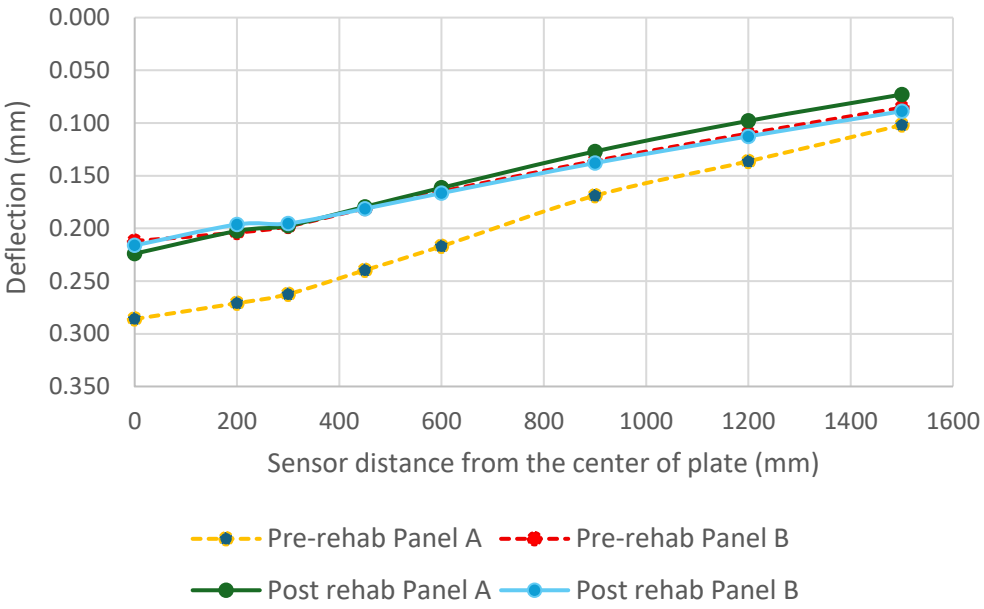

Figure 4.5: Street 2 mid-slab for pre- and post-deflection basin graph



(a) Joint Pre-rehabilitation



(b) Joint Post-rehabilitation



(c) Mid-slab panel: Pre-rehabilitation



(d) Mid-slab panel: Post-rehabilitation

Figure 4.6: Typical Street 2 joints and mid-slab panels of pre- and post-rehabilitation

4.3 Street 3

Table 4.8 highlights the LTE results, performance criteria, and the expected d-cracking severity attributed to each criterion. Table 4.9 presents the pre- and post-rehabilitation mid-span backcalculated modulus for each pavement layer, the corresponding typical range, and an indicator showing whether each layer falls within that range. Table 4.10 lists the identified distresses, affected slabs, and distress density based on the automated distress survey data. Figure 4.7 shows the comparison of pre- and post-rehabilitation of joints with their respective LTE values. Figure 4.8 illustrates the deflection basin graph, showing the pre- and post-rehabilitation deflection response corresponding to sensor distance from the center of load plate. Figure 4.9 presents the typical photographs of the joint and mid-slab locations where the deflection data were collected.

Table 4.8: Load transfer efficiency (LTE) of before and after rehabilitation treatment

Location	Pre-LTE Score (%)	Pre-Performance Rating	Post-LTE Score (%)	Post - Performance Rating	Level of Improvement (%)
Joint 1	69	Good	76	Good	+7
Joint 2	**No testing was conducted**		96	Excellent	-

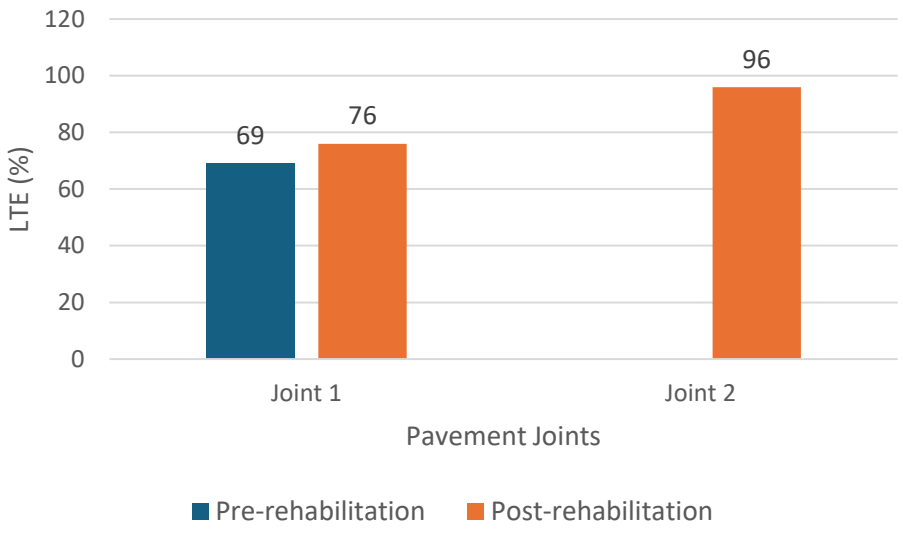

Figure 4.7: Street 3 pre- and post-LTE values at transverse joints

Table 4.11: Mid-slab backcalculated layer properties for pre- and post-rehabilitation treatment

Location	Layer	Thickness (mm)	Backcalculated Modulus (MPa)	Typical range (MPa)	Backcalculation within Tolerance
Pre-rehabilitation values					
Panel A	Rigid slab	150	30,112	20,000 - 35,000	Yes
	Base	75	211	100 - 350	Yes
	Subgrade	0	68	20 - 80	Yes
Post-rehabilitation values					
Panel A	HMA	50	3,000	1,500 - 3,500	Yes
	Rigid slab	150	32,574	20,000 – 35,000	Yes
	Base	75	277	100 - 350	Yes
	Subgrade	0	84	20 - 80	Yes

* Out of typical range, ** Below typical range

Table 4.9: Distresses identified on Street 3 from the automated distress survey

Distress Type	Severity Level	Count of affected Slabs (out of 39)	Distress Density (%)
Durability (D) cracking	L	17	44
	M	19	49
	H	4	10
Faulting	L	43	50
	M	34	40
	H	10	12
Divided slab	L	-	-
	M	-	-
	H	-	-
Linear cracking	L	25	64
	M	-	-
	H	-	-
Joint spalling	L	1	3
	M	1	3
	H	-	-
Corner spalling/ breaking	L	1	3
	M	-	-
	H	-	-

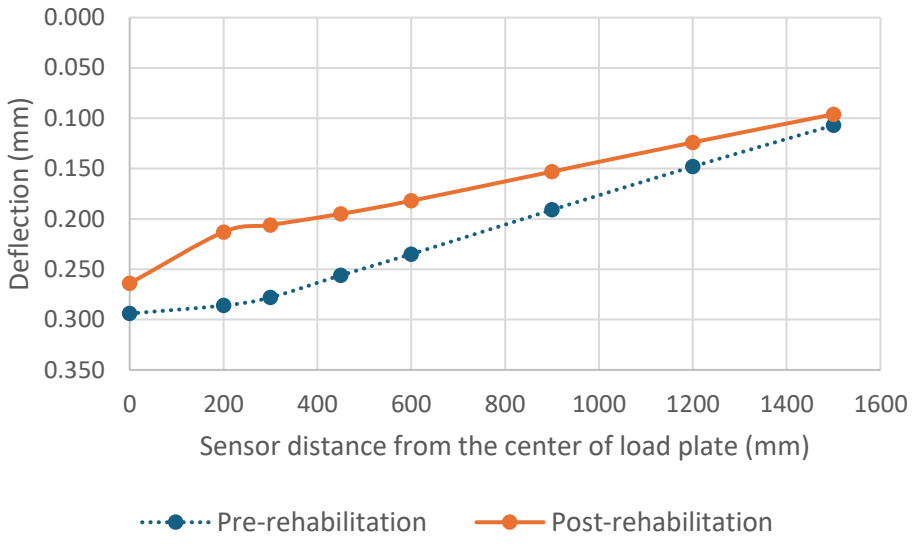

Figure 4.8: Street 3 mid-slab for pre- and post-deflection basin graph

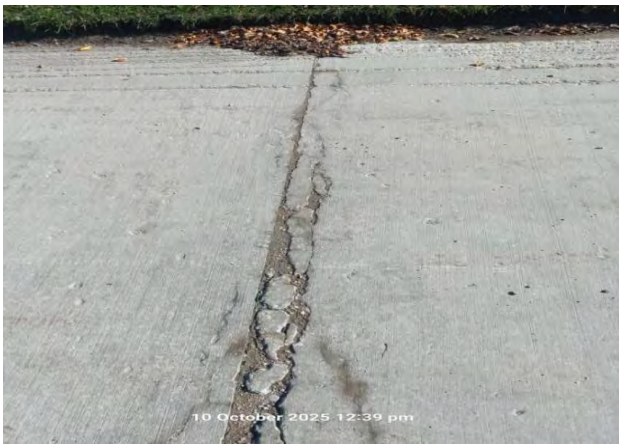

(a) Joint pre-rehabilitation



(b) Mid-slab pre-rehabilitation



(c) Joint post-rehabilitation before overlay



(d) Mid-slab post-rehabilitation before overlay



(e) Joint post-rehabilitation after overlay



(f) Mid-slab post-rehabilitation after overlay

Figure 4.9: Typical Street 3 post-rehabilitation of joint and mid-slab panel

5.0 Conclusions

The study involves site visits to identify candidate pavements affected by d-cracking, collected deflection basin data with FWD testing equipment. The data collected were checked for variability, normalized to a 40 kN and analyzed using BAKFAA software. The results indicated significant variability in LTE, backcalculation, and deflection basin across the 12 tested streets. The LTE, backcalculation moduli and deflection basin are the following:

5.1 Load transfer efficiency

Some joints showed significant improvement (90% & above) and moderate improvement (75% to 89%). Marginal improvement was observed at a joint on street 1 with the LTE pre- and post-values falling within 50% to 74% threshold. This variability can be an indication that the effectiveness of the applied treatments varies across the streets. LTE results allow for the classification of d-cracking severity levels, and dowel performance at transverse joints. Poor LTE can be correlated with increased risk of pumping, faulting, and accelerated distress propagation

5.2 Backcalculated moduli:

The backcalculated modulus for each pavement layer was compared against the typical ranges. The results of backcalculated layer properties for street 1 and 3 indicated an increase in the structural capacity after rehabilitation. The HMA modulus was fixed during the analysis while others were varied. The underlying layer moduli also showed increment results after the rehabilitation.

6.0 The contributions and limitations

Provision of a data-driven residential street pavement management system can enable informed and effective decision-making. Using this data and analysis, municipalities can better prioritize maintenance needs, optimize maintenance budgets and enhance the long-term performance and durability of residential rigid pavements.

The study limitations are:

1. Uneven or surface irregularities may affect load transfer and sensor measurements, which can potentially introduce variability into the measured deflection basins. Although efforts were made to select the most level areas for testing, measurement uncertainty may still exist.

2. The analysis assumes seed (initial) modulus, layer thickness during analysis. Material properties were assumed to be relatively uniform within each pavement layer. In practice, the underlying subgrades may exhibit spatial variability that may not be fully captured during the testing and analysis.

References

ASTM-D4694-90, (2020). *Standard Test Method for Deflections with a Falling-Weight-Type Impulse Load Device.* ASTM International. https://doi.org/10.1520/D4694-09R20

Dam, T. Van, Smith, K., Snyder, M., Ram, P., & Dufalla, N. (2019). FHWA Report: Strategies for Concrete Pavement Preservation. *Federal Highway Administration*.

FHWA. (2017). Using Falling Weight Deflectometer Data with Mechanistic-Empirical Design and Analysis, Volume III: Guidelines for Deflection. Publication no. FHWA-HRT-16-011.

FAA - BAKFAA. Retrieved March 1, 2026, from: https://www.airporttech.tc.faa.gov/Airport-Pavement/Evaluation-Management

US Army Corps of Engineers Construction Engineering Research Laboratory (USACERL). (1997). Paver concrete distress manual. Technical report 97/105. Pavement Distress and Identification Guide for Jointed Concrete Roads and Parking Lots.

Mcleod, H. A. K., Welge, P. E. J., & Robert Henthorne, P. E. (2014). *Aggregate Freeze-Thaw Testing and D-Cracking Field Performance: 30 Years Later*. www.ntis.gov.

Taylor, P., and Wang, X. (2015). Materials-related Distress: Aggregates, Best Practices for Jointed Concrete Pavements, FHWA tech brief FHWA-HIF-15-013.